

## MBE-growth, characterization and properties of InN and InGaN

Y. Nanishi<sup>\*,1</sup>, Y. Saito<sup>1</sup>, T. Yamaguchi<sup>1</sup>, M. Hori<sup>1</sup>, F. Matsuda<sup>1</sup>, T. Araki<sup>1</sup>, A. Suzuki<sup>2</sup>, and T. Miyajima<sup>3</sup>

<sup>1</sup> Dept. of Photonics, Ritsumeikan Univ., 1-1-1 Noji-higashi, Kusatsu 525-8577 Japan

<sup>2</sup> Res. Org. of Sci. and Eng., Ritsumeikan Univ., 1-1-1 Noji-higashi, Kusatsu 525-8577 Japan

<sup>3</sup> Sony Corp. Core Technology & Network Company, 4-14-1 Asahi, Atsugi, Kanagawa 243-0014, Japan

Received 8 May 2003, revised 7 June 2003, accepted 29 June 2003

Published online 7 October 2003

PACS 73.50.Dn, 78.55.Cr, 78.60.Hk, 81.05.Ea, 81.15.Hi

Recent developments on RF-MBE growth of InN and InGaN and their structural and property characterizations are reviewed. For successful growth of high quality InN, (1) nitridation of the sapphire substrates, (2) two-step growth, (3) precise control of V/III ratio and (4) selection of optimum growth temperature are found to be essential. Characterization using XRD, TEM, EXAFS and Raman scattering have clearly demonstrated that InN films have ideal hexagonal wurtzite structure. It is also found that the film has N-polarity. Studies on optimum growth condition dependence on substrate polarity using C and Si face SiC substrates and Ga and N face free-standing GaN substrates are also demonstrated. The result explains why high-quality InN grown by RF-MBE has N-polarity. PL and CL studies on these well-characterized high-quality InN have shown luminescence peaks at approximately 0.75 eV at 77K. These values, however, change slightly depending on measurement temperatures and probably on the residual carrier concentrations. InGaN with full compositional range are also successfully grown on sapphire substrates and band gap energies of these alloys are also studied using PL and CL. Based on these results, true band gap energies of InN are discussed. This paper also includes latest study on single crystalline InN growth on Si (111) substrates.

© 2003 WILEY-VCH Verlag GmbH & Co. KGaA, Weinheim

**1 Introduction** InN is considered to be a very attractive material for future photonic and electronic devices owing to its outstanding material properties like smallest effective mass, largest mobility, highest peak and saturation velocities, and smallest direct band gap in nitride semiconductors. However, until now, InN has been the least studied of nitride semiconductors. This is mainly because of its difficulty in obtaining high quality InN crystals, which is due to the low dissociation temperature and high equilibrium vapor pressure of nitrogen. First successful single crystalline InN growth was reported by Matsuoka et al. in 1989 [1] using metalorganic vapor phase epitaxy (MOVPE). Properties of InN grown by this method have been much improved very recently [2]. MOVPE, however, has an inherent disadvantage because it must satisfy the conditions for NH<sub>3</sub> pyrolysis and prevention of InN dissociation, which impose conflicting temperature requirements.

In contrast, RF-plasma excited molecular beam epitaxy (RF-MBE) has an essential advantage over MOVPE for obtaining high-quality InN. In this growth method, excited nitrogen radicals can be generated separately in a plasma source, enabling us to select growth temperature without considering the requirements of NH<sub>3</sub> pyrolysis. Probably due to the inherent advantage of this growth method, MBE growth studies produced high-quality InN films within a relatively short period of time [3–5] and electri-

\* Corresponding author: e-mail: nanishi@se.ritsumeik.ac.jp, Phone: +81 77 561 2679, Fax: +81 77 561 3994

© 2003 WILEY-VCH Verlag GmbH & Co. KGaA, Weinheim

cal properties with room temperature electron mobility over  $2100 \text{ cm}^2/\text{Vs}$  and residual carrier concentration close to  $3 \times 10^{17}/\text{cm}^3$  are reported very recently [6].

The band gap energy of InN has been well recognized to be 1.9 eV for a long time, after it has been determined by optical absorption using poly-crystalline InN [7, 8]. Very recent studies on PL and optical absorption of single-crystalline InN films grown by MOVPE and MBE, however, have demonstrated that the fundamental band gap of single-crystalline InN should be 0.7–0.8 eV, rather than 1.9 eV [9–12]. After these reports, discussion on the true band gap energy of InN and possible extension of the InN application field attracted much attention.

Back in 1989, Matsuoka et al. [1] have already suggested that single-crystalline InN may have a much smaller band gap than poly-crystalline InN from the band gap energy dependence of InGaN alloys on In composition. A similar possibility of a narrower band gap of InN has also been suggested by Yamaguchi et al. [13] from the band gap energy dependence of InAlN. Following these early suggestions, Inushima et al. reported 1.1 eV as InN band gap energy in 2001 [14]. All these reports before 2002 discussed the InN band gap energy from optical absorption. Recent reports after 2002 [9–12] discussed the InN band gap energy based on luminescence and photo-reflectance studies as well as on optical absorption results. These reports, however, did not involve a detailed study on structural and property relationship.

In this paper, we review recent studies on high-quality InN and InGaN growth by RF-MBE on sapphire substrates. Systematic studies on structural, electrical and optical properties are presented and we will discuss the true band gap energy of InN based on these results. XRD, TEM, CAICISS as well as EXAFS were used for structural characterization. PL, CL and optical absorption were used for optical characterization and Hall measurements were used for electronic characterization.

**2 Critical MBE growth conditions for high-quality InN** An RF-MBE growth system used in this study can be evacuated up to  $1 \times 10^{-10}$  Torr. This MBE system is equipped with a SVTA radical cell (model 2.75) as a nitrogen source. High-purity In and Ga were evaporated from standard effusion cells. The typical growth rate of InN was approximately 500 nm/h. Growth temperatures were carefully monitored with a pyrometer at each growth run.

To guaranty InN single-crystalline growth on sapphire substrates, a nitridation process prior to growth is found to be essential [15]. Without this process, InN tends to grow with both  $[10\bar{1}0]_{\text{InN}} \parallel [11\bar{2}0]_{\text{sapphire}}$  and  $[11\bar{2}0]_{\text{InN}} \parallel [11\bar{2}0]_{\text{sapphire}}$  epitaxial relationships, resulting in the formation of poly-crystalline InN with small grains of both directions. This is due to the fact that lattice mismatch values in these two cases are very close each other. This relationship is a clear contrast to GaN or AlN growth on a sapphire substrate, where the lattice mismatch for the case of  $[10\bar{1}0]_{\text{GaN, AlN}} \parallel [11\bar{2}0]_{\text{sapphire}}$  is much smaller than that of the  $[11\bar{2}0]_{\text{GaN, AlN}} \parallel [11\bar{2}0]_{\text{sapphire}}$  case. With nitridation process, on the other hand, the epitaxial relationship can be uniquely determined to  $[10\bar{1}0]_{\text{InN}} \parallel [11\bar{2}0]_{\text{sapphire}}$ . This is probably due to the formation of an AlN or AlON layer with  $[10\bar{1}0]_{\text{AlN}} \parallel [11\bar{2}0]_{\text{sapphire}}$ , which results in the  $[10\bar{1}0]_{\text{InN}} \parallel [10\bar{1}0]_{\text{AlN}} \parallel [11\bar{2}0]_{\text{sapphire}}$  relationship [15]. X-ray diffraction (XRD) pole-figures of InN grown without and with nitridation process are compared in Fig. 1.

To grow high-quality InN films, obtaining atomically flat surfaces is important. The application of the well-known two-step growth method was found to be very effective for growing flat and high-quality films on the sapphire substrate as in the case of GaN and AlN. The temperature for buffer layer growth, however, should be reduced to approximately 300°C for InN [16]. Consecutive annealing at the growth temperature prior to the main growth process is effective for improving the crystal quality of InN, as evidenced by RBS measurements [17].

The control of the V/III ratio is by far the most important issue to obtain high-quality InN by MBE [18]. At temperatures below the dissociation temperature of InN (approximately 550 °C), the equilibrium vapor pressure of nitrogen molecules over InN is much higher than the In evaporation pressure over In metal [19]. To suppress the dissociation of InN films, one should have a nitrogen pressure higher than the equilibrium pressure during the entire growth process. In order to enhance migration to obtain high-quality films, on the other hand, one should grow InN under slightly In-rich conditions. Considering both limitations for InN MBE growth, the V/III ratio on the surface should be carefully controlled as close as

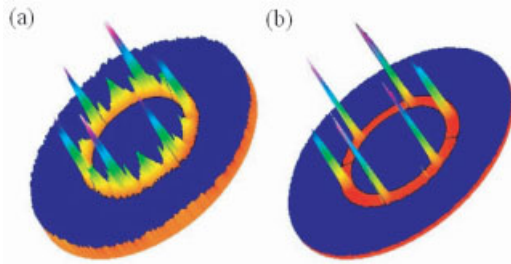


**Fig. 1** XRD pole figures of the InN grown a) with- and b) with nitridation process.

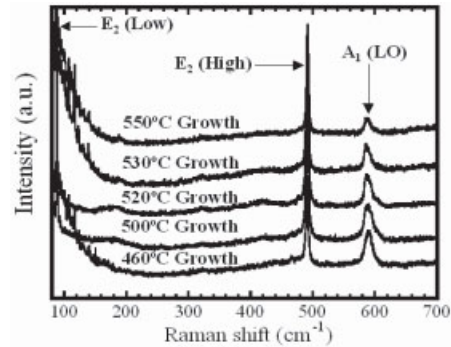


**Fig. 2** Raman spectra for InN films grown at 550 °C, 530 °C, 520 °C, 500 °C and 460 °C.

possible to stoichiometry maintaining the surface slightly N-rich. Otherwise, In droplets should form on the surface and cannot be evaporated from the surface [3].

Optimization of the growth temperature is another critical issue to obtain high-quality InN films. InN films were grown at various growth temperatures between 460 °C and 550 °C and corresponding Raman spectra and PL spectra were compared [12]. Raman spectra of ideal hexagonal wurtzite InN have been obtained (Fig. 2). An FWHM as narrow as 3.7 cm<sup>-1</sup> for the E<sub>2</sub> (high)-phonon-mode was obtained for 550 °C growth. The narrowest FWHM of the E<sub>2</sub> (high)-phonon-mode obtained so far in this study is 3.2 cm<sup>-1</sup>. These results indicated that the crystalline quality was improved by increasing the growth temperature within the dissociation limit of InN.

**3 Structural characterization** For structural characterization,  $\omega$ -scan X-ray diffraction (0002) and (30 $\bar{3}$ 2) rocking curves (XRC) and  $\omega - 2\theta$  scan XRD were carried out. XRC of (0002) diffraction is shown in Fig. 3 and corresponding FWHM is as narrow as 236.7 arcsec, which is comparable to the value obtained from typical MOCVD grown GaN. The FWHM of (30 $\bar{3}$ 2) XRC, on the other hand, was found to be as high as 4500 arcsec [20]. This is attributed to the existence of twisted domains in the film. Figure 4 shows a typical  $\omega - 2\theta$  scan XRD curve, which gives an FWHM of only 28.9 arcsec, indicating an excellent crystallographic quality.

Studies using TEM were also performed for structural characterization [20]. Selected area diffraction patterns confirmed the hexagonal wurtzite structure of InN. The cross-sectional TEM image in Fig. 5 clearly indicates the existence of columnar domains with small angular distribution in the c-plane (twist) and high density of threading dislocations of more than  $2 \times 10^{10}/\text{cm}^2$ . Cross-sectional TEM observations

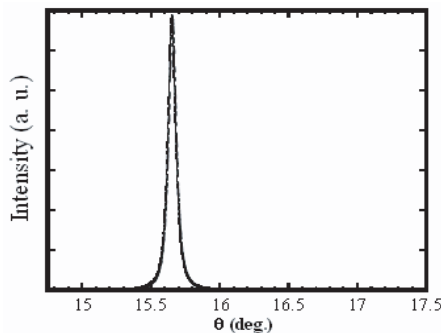


**Fig. 3**  $\omega$ -scan XRC of (0002) InN.

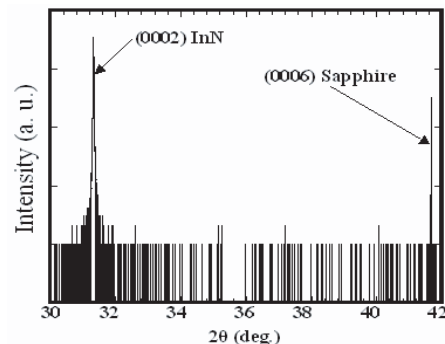


**Fig. 4**  $\omega - 2\theta$  scan XRD curve for InN.

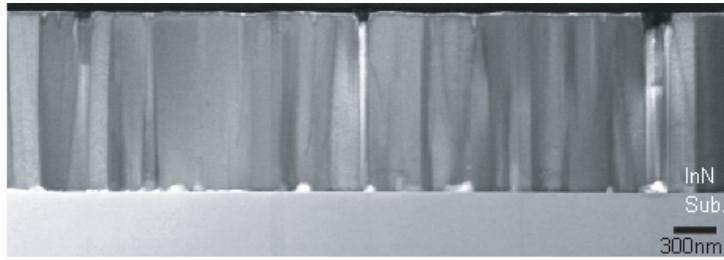


**Fig. 5** Cross-sectional TEM image of InN.

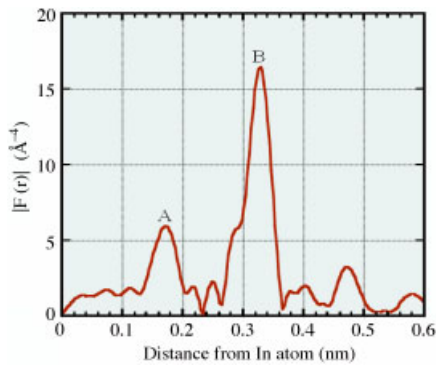


**Fig. 6** (online colour at: www.interscience.wiley.com) Absolute value of radial structure function  $|F(r)|$  around In atoms of InN.

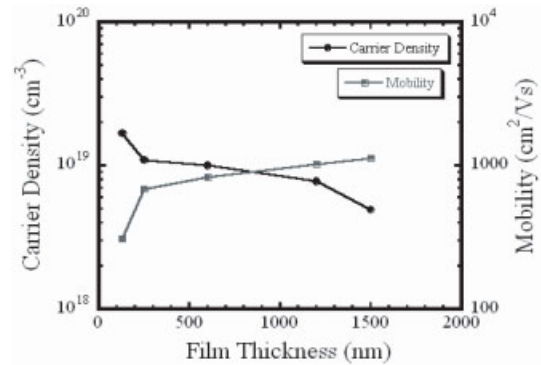


**Fig. 7** Dependence of electrical properties on film thickness.

with a different  $g$  vector of  $1\bar{1}00$  and  $0002$  indicate that most of the dislocations are edge type and those with screw components are relatively small with a density of  $2 \times 10^9/\text{cm}^2$  [20].

The local atomic structure near In atom was investigated using EXAFS oscillations of the In K edge [21]. The signals from the first-nearest neighbor atoms (N) and the second nearest atoms (In) from In atoms were clearly observed as shown in Fig. 6. Atomic distances to the first nearest neighbor atoms and the second nearest neighbor atoms were estimated to be  $d_{\text{In-N}} = 0.214$  nm and  $d_{\text{In-In}} = 0.353$  nm, respectively. Coordination numbers of the first nearest N and the second nearest In atoms were estimated to be 3.7 and 11.8, respectively. The In–In bond length of 0.353 nm is close to their  $a$ -axis lattice constant of 0.3536 nm, which was estimated using XRD. The local atomic structure characterized by EXAFS confirmed  $sp^3$  hybridization bonds of ideal wurtzite InN.

**4 Electrical properties** The electrical properties of the film grown in this study were characterized by Hall effect measurements. InN in and around the buffer layer on the sapphire substrate should contain a lot of defects and the electrical properties in this region should be very poor. By growing films with various thicknesses up to 1.5  $\mu\text{m}$ , we studied the dependence of the electrical properties on film thickness. The results are shown in Fig. 7. Much improvement in electrical properties is obtained with an increase in film thickness. The carrier concentration and room temperature electron mobility of 1.5  $\mu\text{m}$  thick film were  $4.9 \times 10^{18}/\text{cm}^3$  and  $1130 \text{ cm}^2/\text{Vs}$ , respectively [17]. The residual carrier concentration in the grown layer is still very high. The origin of this high residual carrier concentration is not known yet.

**5 Optical properties and discussion on the true band gap energy of InN** The PL spectra obtained from 1.5  $\mu\text{m}$  thick InN at 77 K and room temperature are shown in Fig. 8. Here,  $\text{Ar}^+$  laser at 514.5 nm was used as excitation source and an InGaAs photodetector was used for monitoring luminescence. Very strong and sharp 77 K luminescence was observed at approximately 0.78 eV with an FWHM of 24 meV. The carrier concentration of this sample is approximately  $5 \times 10^{18}/\text{cm}^3$ . It was also confirmed that the

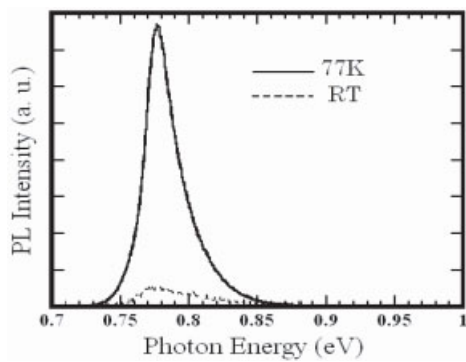


**Fig. 8** PL spectra of InN at 77 K and room temperature.

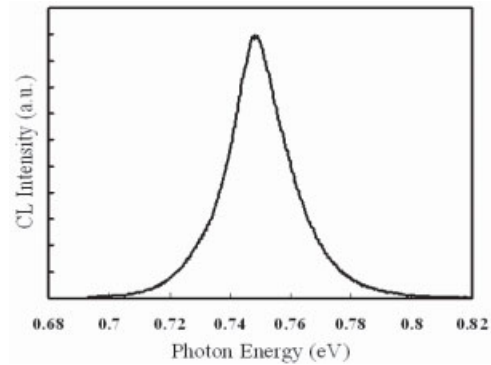


**Fig. 9** CL spectra of InN at 28 K.

wavelength of the PL peak position did not show any noticeable change even if the excitation power was changed over two orders of magnitude from  $65 \text{ mW/cm}^2$  to  $6.5 \text{ W/cm}^2$ . These results suggest that PL should originate from the fundamental interband transition of the InN film. It should be emphasized that no PL corresponding to the 1.9 eV transition could be observed from any InN films grown in this study. The optical absorption of InN was also studied at room temperature. The optical absorption coefficient squared versus the photon energy also suggests that the absorption edge should be less than 0.8 eV [12].

CL is also utilized to characterize the optical properties of the same sample. In this study an, InGaAs photodetector was cooled to 280 K rather than 140 K to extend the detector sensitivity to the longer wavelength region. A Gaussian distribution with a peak at 0.75 eV was observed at 28 K, as shown in Fig. 9.

All of these luminescence studies suggested that the true band gap energy of well-characterized InN samples grown in the study should be approximately 0.75 eV at 77 K and slightly smaller at room temperature. However, the value changes slightly among the samples, probably depending on the variation of the residual carrier concentration. For accurate determination of the true band gap energy of InN, further reduction of the residual carrier concentration should be needed. The origin of the 1.9 eV band gap energy is still open for discussion. Several possibilities were pointed out so far including, (1) influence of oxygen incorporation or formation of alloys with  $\text{In}_2\text{O}_3$ , (2) quantum size effect of polycrystallites and (3) boundary effect of polycrystalline grains.

InGaN films with the entire alloy composition were successfully grown on sapphire substrates by inserting a low-temperature-grown InN buffer layer. Unlike in the case of MOVPE, the solid composition can be simply determined by the In/Ga flux ratio [22]. Peak positions of CL and PL spectra at 77 K

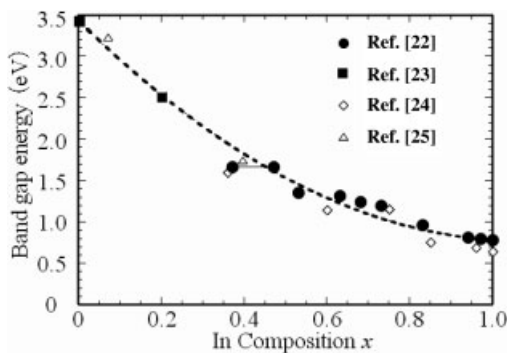


**Fig. 10** Peak position of CL and PL spectra at 77 K as a function of In composition in InGaN alloys.

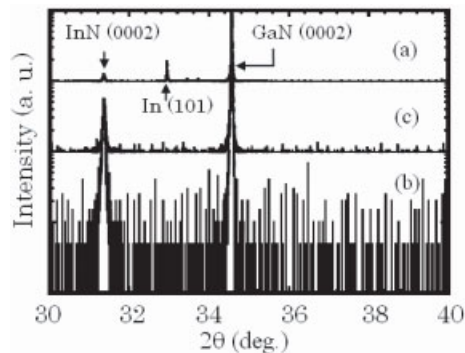


**Fig. 11** Typical  $\omega-2\theta$  XRD profiles of InN grown on a) Ga-face GaN at 550 °C, b) N-face GaN at 550 °C and c) Ga-face GaN at 450 °C.

as a function of In composition are shown in Fig. 10. This figure also supports that the band gap energy of InN should be approximately 0.75 eV at 77 K.

**6 Crystal polarity and its influence on growth conditions** Studies on the polarity of InN by CAICISS [26], the convergent beam electron diffraction method by TEM [20], as well as chemical etching revealed that high-quality InN films grown on sapphire substrate have always N-polarity. InN growth studies on the substrates with well controlled polarity, like Si-face and C-face SiC substrates and Ga-face and N-face free-standing GaN substrates have clearly demonstrated that InN can be grown at higher temperatures on N-polarity substrate than Ga-polarity substrate and In droplets easily form on Ga-polarity substrate [27]. This experimental result can be explained by the difference in bonding configuration of the topmost N atoms between the two cases. For InN growth with In-polarity, N atoms sit on the surface with one bondings to In atoms. On the other hand, N atoms sit on the surface with three bonding to In atoms for the growth with N-polarity. It is easily expected that the desorption of nitrogen occurs more easily in the InN growth with In-polarity, resulting in the easy formation of In droplets.

Typical  $\omega - 2\theta$  XRD profiles of InN grown at 550 °C with the same V/III ratio on (a) Ga-face GaN and (b) N-face GaN were compared in Fig. 11. This figure also indicates that InN can be grown on Ga-face GaN if the growth temperature was reduced to 450 °C. The crystal quality of InN grown on N-polarity substrate (case (b)), however, is better than on Ga-polarity substrate (case (c)), because the growth temperature for the former case is higher than in the latter case [27].

Thus, the ability to incorporate nitrogen to the growing surface is essential for successful growth of InN. This ability is much higher when they are grown with N-polarity, enabling us to grow at higher temperatures than the growth with In-polarity.

**7 InN growth on Si substrate** We have successfully grown single-crystalline InN films on (111) Si substrates for the first time by a brief nitridation (3 min) of Si substrates prior to growth and the following low-temperature buffer layer deposition [28]. The band gap energy of a single-crystalline hexagonal InN films grown on a Si substrate was estimated to be approximately 0.8 eV from PL measurements. Prolonged nitridation for 30 min have resulted in the formation of polycrystalline InN. This is probably due to the formation of amorphous SiN on Si (111) substrates. We have observed, however, strong photoluminescence even from this polycrystalline InN, with a luminescence peak again at approximately 0.8 eV [29]. Yodo et al. reported 1.9 eV PL from InN grown on Si substrates [30]. The result obtained in this study implies that the origin of the 1.9 eV luminescence is related neither to Si substrates nor to polycrystal formation of InN.

**8 Conclusion** Systematic studies on InN RF-MBE growth and characterization have been carried out. (1) Nitridation of the sapphire substrates, (2) two-step growth, (3) precise control of the V/III ratio and (4) selection of the optimum growth temperature are pointed out as critical conditions to obtain high-quality InN. Structural characterizations using XRD, TEM and EXAFS have clearly demonstrated that InN films have ideal hexagonal wurtzite structure. CAICISS and convergent beam electron diffraction studies also revealed that these high-quality InN films have N-polarity. FWHMs of  $\omega - 2\theta$  mode XRD and  $E_2$  (high)-phonon-mode of Raman scattering were as small as 28.9 arcsec and 3.2  $\text{cm}^{-1}$ , respectively. TEM study revealed, however, that these InN films contain columnar domains with small angular distribution in the  $c$ -plane and high density of threading dislocations with density as high as  $2 \times 10^{10}/\text{cm}^2$ . Electrical characterization indicated room temperature electron mobilities over 1100  $\text{cm}^2/\text{Vs}$ . However, a high density of residual carriers in the middle of  $10^{18}/\text{cm}^3$  still exists in the films. Although InN films still contain a high density of defects, they show sharp and strong luminescence by PL and CL observations. These luminescences are considered to originate from the fundamental interband transition. These results indicated that the band gap of well-characterized single-crystalline InN should be approximately 0.75 eV at low temperatures. For determination of the accurate band gap energy of InN, however, further reduction in residual carrier concentration should be needed. As it has become clear that the fundamental band gap of InN should be approximately 0.75 eV, new application

fields should open up as new light sources, high efficiency solar cells and high-power, high-frequency electronic devices.

**Acknowledgements** The authors would like to thank H. Harima for Raman scattering measurements. This work was supported by the Ministry of Education, Culture, Sports, Science and Technology, Grant-in-Aid for Scientific Research (B) #13450131, Academic Frontier Promotion Project and The 21st Century COE Program.

## References

- [1] T. Matsuoka, H. Tanaka, and A. Katsui, Int. Symp. on GaAs and Related Compounds, Karuizawa, 1989, Inst. Phys. Conf. Ser. **106**, 141 (1990).
- [2] A. Yamamoto, T. Tanaka, K. Koide, and A. Hashimoto, phys. stat. sol. (b) **194**, 510 (2002).
- [3] Y. Saito, N. Teraguchi, A. Suzuki, T. Araki, and Y. Nanishi, Jpn. J. Appl. Phys. **40**, L91(2001).
- [4] M. Higashiwaki and T. Matsui, Jpn. J. Appl. Phys. **41**, L540 (2002).
- [5] H. Lu, W. J. Schaff, J. Hwang, H. Wu, G. Koley, and L. F. Eastman, Appl. Phys. Lett. **79**, 1489 (2001).
- [6] H. Lu, W. J. Schaff, L. F. Eastman, J. Wu, W. Walukiewicz, D. C. Look, and R. J. Molnar, Mater. Res. Soc. Symp. Proc. **743**, L4.10 (2003).
- [7] K. Osamura, K. Nakajima, and Y. Murakami, Solid State Commun. **11**, 617 (1972).
- [8] T. L. Tansley and C. P. Foley, J. Appl. Phys. **59**, 3241(1986).
- [9] V. Y. Davydov, A. A. Klochikhin, R. P. Seisyan, V. V. Emtsev, S. V. Ivanov, F. Bechstedt, J. Furthmuller, H. Harima, A. V. Mudryi, J. Adrhold, O. Semchinova, and J. Graul, phys. stat. sol. (b) **229**, R1 (2002).
- [10] T. Matsuoka, H. Okamoto, M. Nakao, H. Harima, and E. Kurimoto, Appl. Phys. Lett. **81**, 1246 (2002).
- [11] J. Wu, W. Walukiewicz, K. M. Yu, J. W. Arger III, E. E. Haller, H. Lu, W. J. Schaff, Y. Saito, and Y. Nanishi, Appl. Phys. Lett. **80**, 3967 (2002).
- [12] Y. Saito, H. Harima, E. Kurimoto, T. Yamaguchi, N. Teraguchi, A. Suzuki, T. Araki, and Y. Nanishi, phys. stat. sol. (b) **234**, 796 (2002).
- [13] S. Yamaguchi, M. Kariya, S. Nitta, T. Takeuchi, C. Wetzel, H. Amano, and I. Akasaki, Appl. Phys. Lett. **76**, 876 (2000).
- [14] T. Inushima, V. V. Mamutin, V. A. Vekshin, S. V. Ivanov, T. Sakon, and S. Motokawa, J. Cryst. Growth **227** 481 (2001).
- [15] T. Yamaguchi, Y. Saito, K. Kano, T. Araki, N. Teraguchi, A. Suzuki, and Y. Nanishi, Proceedings of Int. Conf. on Indium Phosphide and Related Materials PII-41, 643 (2002).
- [16] Y. Saito, N. Teraguchi, A. Suzuki, T. Araki, and Y. Nanishi, IPAP conf. Series. **1**, 182 (2000).
- [17] Y. Nanishi, Y. Saito, and T. Yamaguchi, Jpn. J. Appl. Phys. **42**, 2549 (2003).
- [18] Y. Saito, N. Teraguchi, A. Suzuki, T. Yamaguchi, T. Araki, and Y. Nanishi, Mater. Res. Symp. Proc. **639**, G11.18 (2001).
- [19] S. V. Ivanov: to be published in Nitride Semiconductors (Hand book on Materials and Devices), edited by P. Ruterana, M. Albrecht, and J. Neugebauer (Wiley-VCH).
- [20] T. Araki, K. Mizuo, T. Yamaguchi, Y. Saito, and Y. Nanishi, ICNS-5, Tu-P2.102 (2003).
- [21] T. Miyajima, Y. Kudo, K. L. Liu, T. Uruga, T. Honma, Y. Saito, M. Hori, Y. Nanishi, T. Kobayashi, and S. Hirata, phys. stat. sol. (b) **234**, 801 (2002).
- [22] M. Hori, K. Kano, T. Yamaguchi, Y. Saito, T. Araki, Y. Nanishi, N. Teraguchi, and A. Suzuki, phys. stat. sol. (b) **234**, 750 (2002).
- [23] C. Wetzel, T. Takeuchi, S. Yamaguchi, H. Katoh, H. Amano, and I. Akasaki, Appl. Phys. Lett. **73**, 1994 (1998).
- [24] V. Y. Davydov, A. A. Klochikhin, V. V. Emtsev, S. V. Ivanov, V. V. Vekshin, F. Bechstedt, J. Furthmuller, H. Harima, A. V. Mudryi, A. Hashimoto, A. Yamamoto, J. Adrhold, J. Graul, and E. E. Haller, phys. stat. sol. (b) **230**, R4 (2002).
- [25] K. P. O'Donnell, J. F. W. Mosselmanns, R. W. Martin, S. Pereira, and M. E. White, J. Phys. Condens. Mater. **13**, 6977 (2001).
- [26] Y. Saito, T. Yamaguchi, H. Kanazawa, K. Kano, T. Araki, Y. Nanishi, N. Teraguchi, and A. Suzuki, J. Cryst. Growth **237–239**, 1017 (2002).
- [27] F. Matsuda, Y. Saito, T. Muramatsu, T. Yamaguchi, Y. Matsuo1, A. Koukitu1, T. Araki, and Y. Nanishi, ICNS-5, Tu-P2.099 (2003).
- [28] T. Yamaguchi, K. Mizuo, Y. Saito, T. Noguchi, T. Araki, Y. Nanishi, T. Miyajima, and Y. Kudo, Mater. Res. Soc. Symp. Proc. **743**, L3.26 (2002).
- [29] K. Mizuo, T. Yamaguchi, Y. Saito, T. Araki, and Y. Nanishi, Mater. Res. Soc. Symp. Proc. **743**, L11.26 (2003).
- [30] T. Yodo, H. Yona, H. Ando, D. Yosei, and Y. Harada, Appl. Phys. Lett. **80**, 968 (2002).